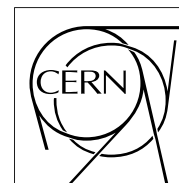**The Compact Muon Solenoid Experiment**

CMS Note

Mailing address: CMS CERN, CH-1211 GENEVA 23, Switzerland

08/09/2000

Study of radiation damage and substrate resistivity effects from beam test of silicon microstrip detectors using LHC readout electronics.

M. M. Angarano, M. Biasini, G.M. Bilei, M.T. Brunetti, B. Checcucci, D. Creanza, M. de Palma, L. Fanò, L. Fiore, M. Giorgi, P. Lariccia, G. Maggi, G. Mantovani, G. Messina, S. My, A. Papi, V. Radicci, R. Santinelli, G. Selvaggi, L. Servoli, L. Silvestris, P. Tempesta

INFN and Dip. Interateneo di Fisica, Bari, Italy

INFN and University of Perugia, Perugia, Italy

Abstract

We present beam test results on single sided silicon microstrip detectors, with different substrate resistivities. The effects of radiation damage are studied on a detector irradiated at a fluence of $2.4 \cdot 10^{14}$ n/cm^2. The detectors are read out with the APV6 chip, which is compatible with the 40 MHz LHC clock. The performance of different detectors and readout modes are studied in terms of signal-to-noise ratio and efficiency.

1   Introduction

The tracking system of the CMS experiment at the future LHC collider, based on silicon mictrostrip detectors, will be exposed to ionizing radiation with an equivalent fluence up to about $1.6 \cdot 10^{14}$ n/cm^2 after 10 years of operation[1] at a radial distance of 22 cm from the interaction point. This irradiation will affect the most important detector parameters, which conversely will give a degradation of detector performances, namely the noise level and the charge collection. Previous studies on electrical performance of microstrip detectors[2] have indicated the advantages of using substrates with low resistivity (1-4 KΩ·cm), related to the possibility of mantaining a relatively low bias voltage after the type-inversion due to radiation damage.

In this paper we investigate the performances on muon beam of p^+ on n-type detectors with different substrate resistivity, before and after irradiation. In addition, the APV6 chip is used as 25ns front-end electronic, and a comparison between the two foreseen readout modes is presented. The attention is focused on signal-to-noise ratio and efficiency for the different resistivities, irradiation and readout modes.

2   Detectors description

The detectors here studied are $< 111 >$ single sided, AC coupled, with p^+ strips 18 μm width, implanted over an n type substrate, produced by CSEM. The active area of the detector is 57.4×57.4 mm^2, the thickness is about 300 μm. The total number of strips is 1024 and the pitch is 61 μm. Two types of detectors with different resistivity are used: 1-2 kΩ·cm (Low Resistivity) and 4-8 kΩ·cm (High Resistivity). The bias is obtained through 2MΩ polysilicon resistors.
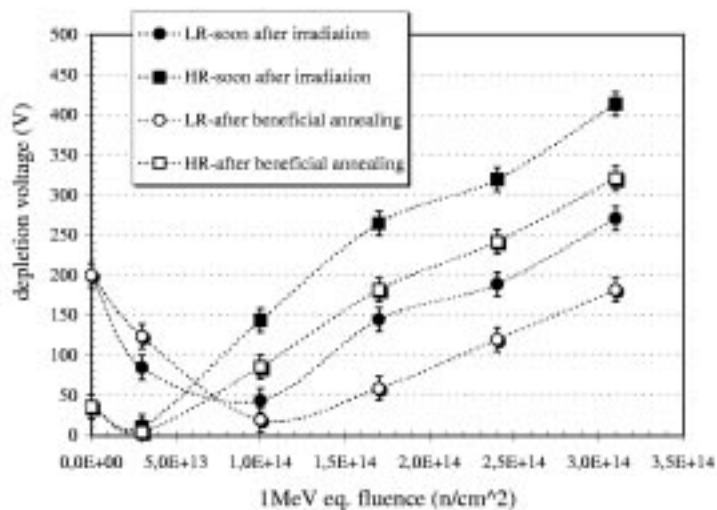

Figure 1: Depletion voltage as a function of fluence: LR vs. HR comparison.

Before irradiation, a low resistivity device has a relatively high value of effective doping concentration (N_{eff}), and therefore a high depletion voltage ($V_{dep} \propto N_{eff}$). The inversion fluences ϕ_{inv} (defined as the fluences at which an n-type silicon becomes "effectively" p-type) depends on N_{eff} as this empirical formula shows:

$$\phi \simeq (17 \div 20) N_{eff}$$

where ϕ_{inv} is expressed in cm^{-2} and N_{eff} in cm^{-3}. As shown in figure 1 [2][1], the low resistivity device compared to the high resistivity one, has the type inversion at larger fluences and the depletion voltage, after the type inversion, lower than one hundred Volts at the same fluence.

Two detectors are bonded together to form a single readout module of about 12 cm length equipped with 2 APV6 chips in the central zone to readout 256 strips. Three modules have been assembled: one with high resistivity substrate (HR-NI), one with low resistivity substrate (LR-NI) and a last one (LR-IR), low resistivity, irradiated with a dose of 2.4×10^{14} n/·cm^2. Irradiation was performed at the ENEA facility in Casaccia (Roma), at room temperature and without biasing the detectors. To avoid anti-annealing effects, the detectors, after irradiation, are kept at a temperature $\simeq -10$ °C.

---

[1] The first set of measures was performed just after irradiation, the second one, after benefical annealing, 15-days after.

3   APV6 Description

The APV6 chip[4] is equipped with 128 analog channels, each one containing a pipeline memory with 160 locations. The two pointers for read-write operation are driven by the 40MHz LHC clock, and are separated by a time interval called *latency*.

There are two different operation modes for the APV6: *peak* and *deconvolution*. In the first case a full sampling of the signal is done, and the fall time for the signal reconstruction is 100ns; in deconvolution mode only 3 samples are needed and the fall time is reduced to 25ns. The introduction of a deconvolution filter gives an increase of about 40% for the electronic noise and a charge loss of about 20%[5].

The APV6 response can be fine tuned using different programmable registers as shown in table 1. An example of this kind of studies will be shown in section 6.

Table 1: Internal APV6 registers

$Register$	$Class$	$Range$	$Resolution$	$Default$
$IPRE$	I	$0 - 1020\,\mu A$	$4\,\mu A$	$440\,\mu A$
$ISHA$	I	$0 - 255\,\mu A$	$1\,\mu A$	$88\,\mu A$
$IPSP$	I	$0 - 127.5\,\mu A$	$0.5\,\mu A$	$42\,\mu A$
$VPRE$	V	$VDD - VSS$	$18\,mV$	$-0.7\,V$
$VSHA$	V	$VDD - VSS$	$18\,mV$	$2.0\,V$
$VADJ$	V	$GND - VSS$	$9\,mV$	$200\,\mu A$
$VCAS$	V	$GND - 1.02\,V$	$4\,mV$	$0\,V$
$CLVL$	Q	$0 - 15.3\,fC$	$0.06\,fC$	Off

IPRE	Preamplifier bias current	ISHA	Shaper bias current
IPSP	APSP bias current	VPRE	Preamplifier feedback bias voltage
VSHA	Shaper feedback bias voltage	VADJ	Output level adjustment
VCAS	Cascade voltage bias level	CLVL	Reference for internal test system

4   Experimental setup

The modules are placed inside a thermally insulated box in wich nitrogen is flushed. The temperature is set at -10°C and monitored to be stable within ±1°C. The modules are readout by a VME-based DAQ system [6]. The detectors are biased in a range up to about 3 times the depletion voltage. The measured depletion voltage is V_d=40, 150, 200 Volts for HR-NI, LR-IR and LR-NI.

The modules are tested using a 100GeV muon beam at X5 CERN area. The trigger is defined by the coincidence of 2 scintillators placed in front of the detectors. The active area of the 2 scintillators is 2x2 cm^2 in the first part of the data taking and 6x6 cm^2 in the second one. No precise tracking is performed during the acquisition due to the absence of the telescope system. Several million triggers were collected during about 10 days of experiment.

5   Analysis method

The data analysis is performed using the ORCA package, developed at CERN by the CMS collaboration [7]. The strip signal (S_i) is calculated from the raw digital value subtracting the strip pedestal and the common mode fluctuation. The strip noise (N_i) is calculated as the statistical fluctuation of the strip signal, excluding the hits caused by a particle. When strip signal and noise are defined the program try to find a cluster. The strips for which the ratio S_i/N_i is greater than a threshold T_s are identified as seed of a possible cluster. The neighbouring strips are associated to the cluster if their ratio S_i/N_i is greater than T_n. For N strips selected in this way, the cluster signal (S_{cl}) and cluster noise (N_{cl}) are calculated as:

$$S_{cl} = \sum_{i=1}^{N} S_i \qquad\qquad N_{cl} = \frac{S_{cl}}{\sum_{i=1}^{N} \dfrac{S_i}{N_i}}$$

Finally, if the signal-to-noise ratio S_{cl}/N_{cl} exceeds the value T_c, the cluster is considered for further analysis. The values used for the cluster finding thresholds are: T_s=4, T_n=2 and T_t=5.
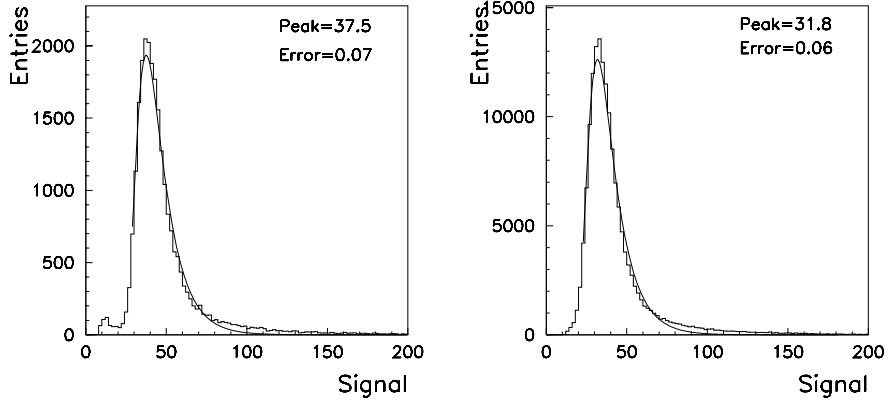
Figure 2: Cluster signal in peak (left) and deconvolution mode (right)
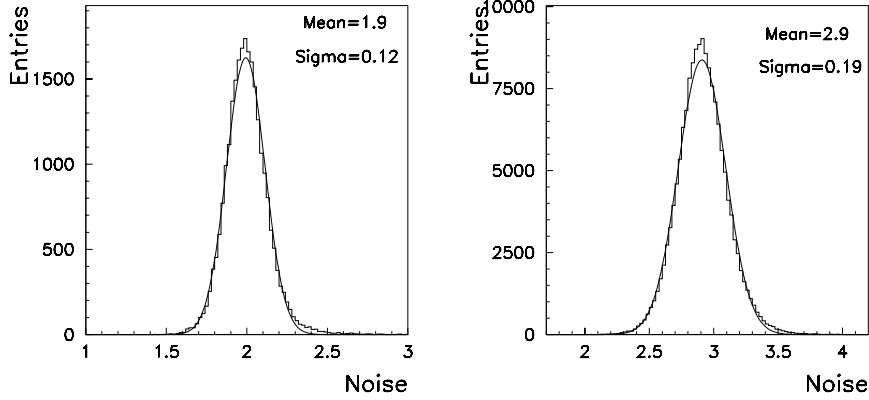

Figure 3: Cluster noise in peak (left) and deconvolution mode (right)

The most probable value of the Landau function which best fits the S_{cl} distribution defines the detector signal, while the most probable value of the Gaussian function fitting the N_{cl} distribution defines the detector noise (figures 2 and 3).

6 Experimental results

6.1 APV6 parameters

The dependence of the detectors performance on the APV6 parameters is studied through a variation of the latency and of the shaper feedback bias voltage, VSHA. For the other parameters of the chip the defaults settings are used.

Fig. 4 a) shows the S/N for the high resistivity not irradiated detector (HR-NI) versus the latency value, for both APV6 operational modes: peak and deconvolution. The two signal-to-noise maximum values are separated in time by 3 latency units (1 latency unit = 25 ns) plus 8ns, as expected [8]. The low-resistivity, irradiated and not irradiated (LR-IR and LR-NI) detectors, exhibit the same time difference. For deconvolution mode, the width of the distribution is narrower with respect to the one for peak mode, for all three kinds of detectors (e.g. figure 4 for the HR-NI detector). This behaviour confirms that the signal sampling time is particularly important for the charge collection optimization in deconvolution mode.

From the study done by varying the parameter VSHA for the HR-NI detector, an increase of the cluster signal is found for increasing values of VSHA (see figure 5). The VSHA parameter seems have no effect on the cluster noise. The percentage increase of the signal, from the minimum to the maximum value of VSHA, is about 45% in peak mode and 14% in deconvolution mode.
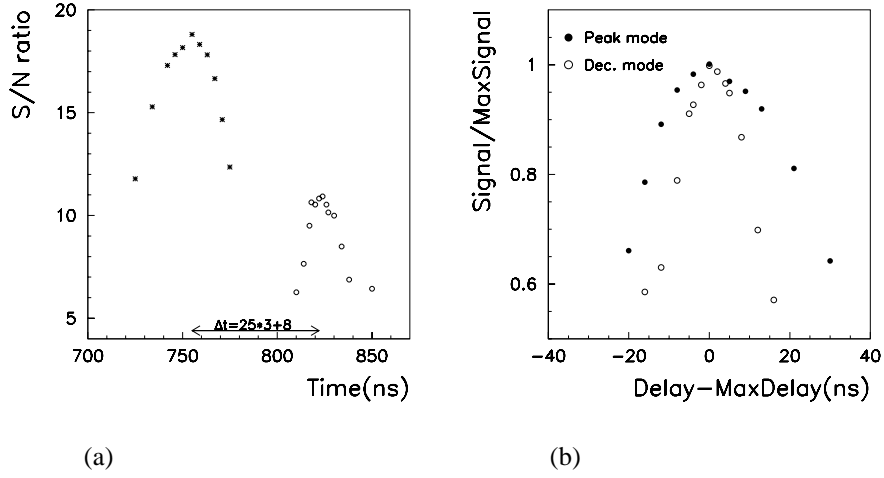
Figure 4: Signal-to-noise ratio as a function of the latency (a) in peak and deconvolution mode (full and empty circles, respectively) for the HR-NI detector. Relative signal for the HR-NI detector as a function of latency subtracted delay (b) for both readout modes.
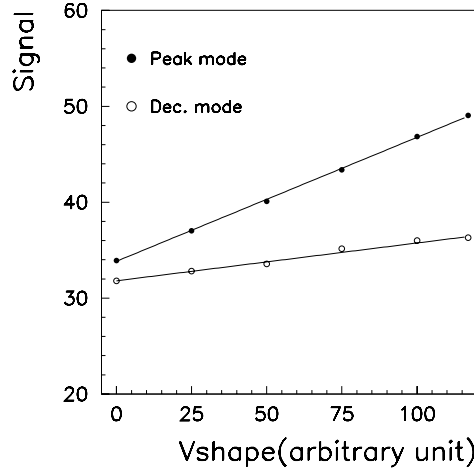

Figure 5: Cluster signal as a function of the VSHA register for the HR-NI detector, in peak and deconvolution mode (black and white circles, respectively)

6.2 Cluster noise and signal-to-noise ratio

A simple theoretical model is used to estimate the signal-to-noise value taking into account the main noise sources in a silicon detector coupled with the front-end electronics: the amplifier noise, the shot noise of the strip leakage current I_s, the thermal noise due to the bias resistor R_{pol} and metal resistance R_s [9]. The analytical formulas of each component are reported in table 2. The total noise, expressed in terms of an equivalent noise charge (ENC), is the sum in quadrature of the four noise sources. Not all the released charge is readout by the electronics because of the AC coupling capacitor. The signal-to-noise ratio can be calculated assuming the injected fractional charge equal to $22400e^-$.

For the noise calculation, we use the values of resistance and leakage current measured in laboratory. C_{tot} can be calculated from:

$$\frac{1}{C_{tot}} = \frac{1}{C_{ac}} + \frac{1}{C_{back} + 2(C_{ii} + C_{ii+1})}$$

where C_{ac} is the coupling capacitance, C_{ii} is the interstrip capacitance, C_{ii+1} is the second neighbour interstrip

5

Noise source	Type	Expression at t=-10C	Deconvolution
Strip leakage current I_b	Parallel	$\simeq 108\sqrt{\tau(ns)I_s(\mu A)}e^-$	x 0.45
Polarization resistors R_p	Parallel	$\simeq 22.5\sqrt{\frac{\tau(ns)}{R_{pol}(M\Omega)}}e^-$	x 0.45
Metal strip resistance R_s	Series	$\simeq 13C_{tot}\sqrt{\frac{R_s(\Omega)}{\tau(ns)}}e^-$	x 1.45
Front-end electronics	Series	$510 + 36C_{tot}$	$1000 + 46C_{tot}$

Table 2: Noise sources. C_{tot} is the total capacitive load seen from the amplifier input into the detector, τ is the shaping time.

capacitance and C_{back} is the backplane capacitance. Before irradiation we can assume that the $C_{tot} \simeq 13pF$ for the high and low resistivity detector; after irradiation $C_{tot} \simeq 19pF$ at V_{dep} and $C_{tot} \simeq 17pF$ at $V_{bias} \sim 2V_{dep}$. As expected from the APV characteristics, the noise is higher in deconvolution than in peak mode. In table 3, we compare the calculated and the measured signal-to-noise ratio. Even if the model used is very simple, we obtain a substantial agreement between measurements and calculations in each configuration.

	Before irradiation		After irradiation	
	peak	deconvolution	peak	deconvolution
Expected	21.4	13.4	14.	11.6
Measured	18.7	12.	13.	8.7

Table 3: Comparison between the estimated and measured signal-to-noise ratios for the low resistivity detectors.

6.3 η-function

In order to check the charge sharing between adjacent strips, the charge of the two strips in the cluster with highest signal is studied. Figure 6 shows the distribution of the response function $\eta = Q_l/(Q_l + Q_r)$, where Q_l and Q_r are the charges collected by the two strips, according to readout order. The distributions for clusters with one, two and three strips are compared, both for peak and deconvolution mode. In all cases the distributions are nearly symmetric, as expected.
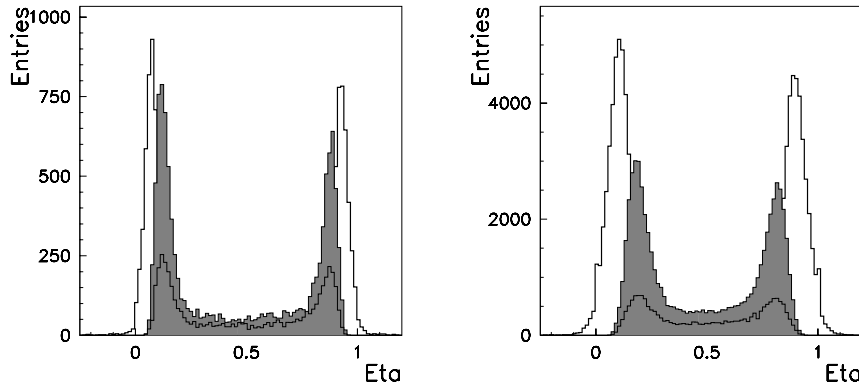

Figure 6: Distribution of the response function η for the high resistivity detector in peak (left) and deconvolution mode (right); black = 1 strip cluster, dashed = 2 strip clusters, dark = 3 strip clusters

6.4 Bias scan

The behavior of the detectors is tested for different values of the bias voltage. This scan is done for all detectors in peak mode and for low-resistivity detectors in deconvolution mode too. We have studied the dependence on bias voltage of signal, noise, signal-to-noise ratio, mean cluster width and detection efficiency.

We have verified that the low resistivity detectors can operate up to 500 V [1] before and after irradiation. As shown in fig.7, the cluster noise does not depend on applied voltage, as expected. The dependence of cluster signal
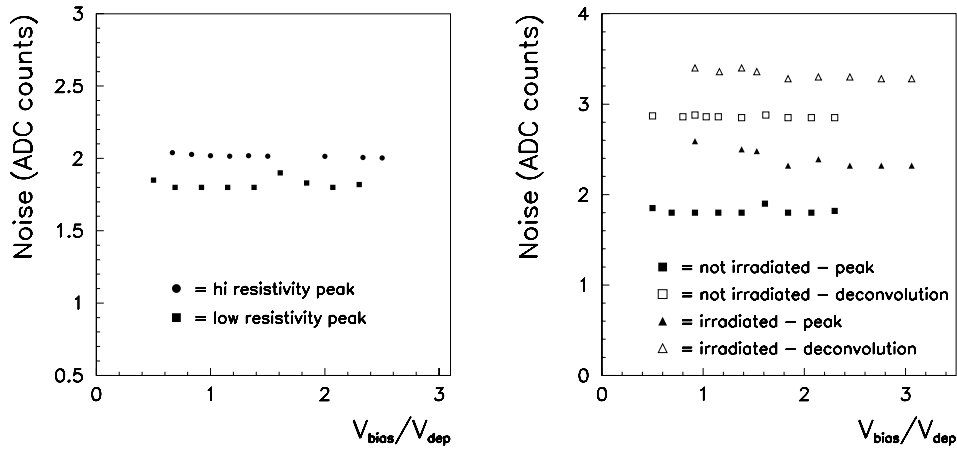
Figure 7: - Left - Cluster noise vs V_{bias}/V_{dep} for HR-NI and LR-NI in peak mode - Right - Cluster noise vs V_{bias}/V_{dep} for LR-NI, LR-IR in peak and deconvolution mode
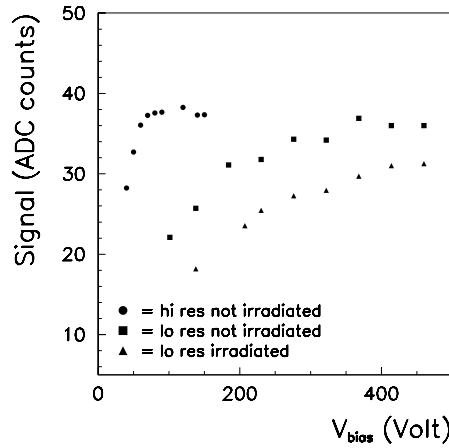

Figure 8: Cluster signal in peak mode as a function of bias voltage for HR-NI, LR-NI and LR-IR modules

on the bias voltage is shown in figure 8. The signal increases with increasing bias voltage, up to a plateau value reached at $\simeq 1.5V_{dep}$. The high resistivity detector shows a uniform behavior for large values of the bias scan, therefore it is operated only up to 150 V. The irradiated detector shows a lower collected charge, of about 20% with respect to not irradiated ones, as expected from radiation damages [1]. Detectors with different resistivities do not present significant differences in performances, as can be inferred from figure 9; the signal-to-noise behavior is very similar for the two detectors, and in agreement with theoretical estimates. In deconvolution mode the detectors have signal-to-noise ratio lower than in peak mode (figure 9) due to the increased noise given by the deconvolution filter [5]. The results obtained in deconvolution mode for the irradiated sensors show the capability of operating the detectors after 15 years of LHC, despite the reduced signal-to-noise ratio with respect to initial performances.

6.5 Cluster size

The size of a cluster is mainly determined by the strip pitch, the interstrip capacitance and by the diffusion length of the electrons. Figure 10 shows the mean cluster width for the different detectors studied. The typical dependence of the interstrip capacitance on the bias voltage is reflected here on the cluster width variation as a function of $(V_{bias}-V_{dep})/V_{dep}$.

For the irradiated detector there is a larger dependence on the bias voltage due to the larger dependence of the interstrip capacitance on the bias voltage. The variation of the interstrip capacitance, due to radiation damage,
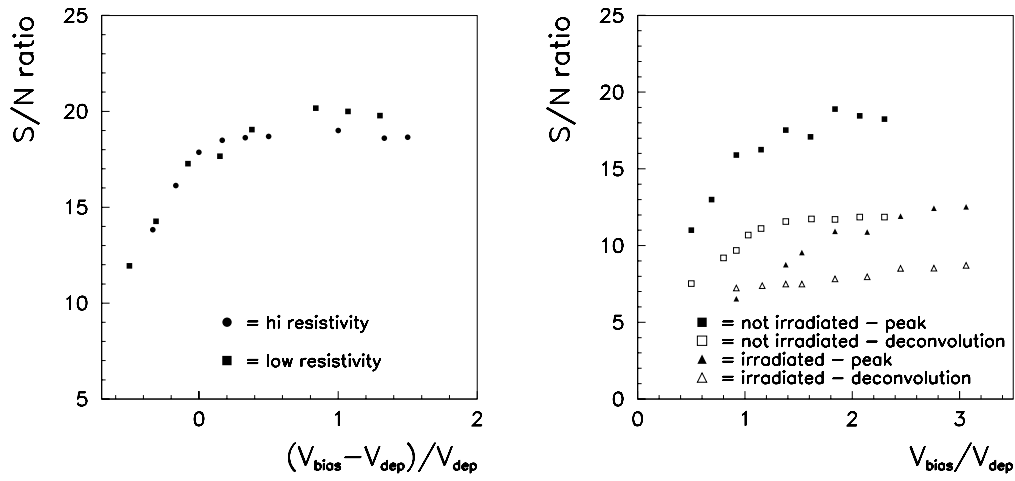
7

Figure 9: Signal-to-Noise ratio as a function of $V_{(bias}$-$V_{dep})/V_{dep}$ for the detectors HR-NI, LR-NI in peak mode on the left and for LR-IR, LR-NI in peak and deconvolution mode on the right

gives rise to the increase of the mean cluster width of the irradiated detector, with respect to the non irradiated one with the same resistivity. The mean cluster width for detectors in deconvolution mode is found to be larger than in peak mode; this can be possibly explained by the increase of the noise in deconvolution mode, which gives a larger probability for neighbour strips to be included in the cluster.
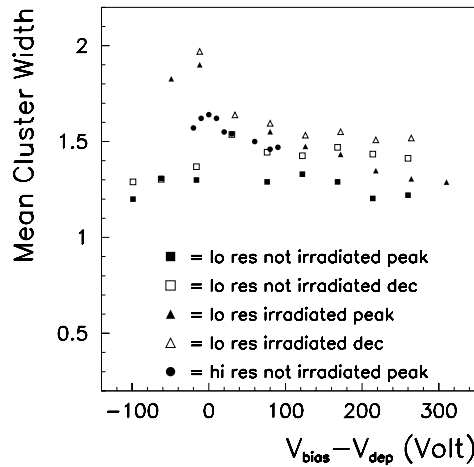

Figure 10: Mean cluster width as a function of V_{bias}-V_{dep} for the HR-NI (circle), LR-NI (box) and LR-IR (triangle) modules in peak (solid) and deconvolution (empty) mode.

6.6 Efficiency

Due to the absence of a high resolution telescope along the beam line, it is not possible to determine the impact position of the tracks on the detectors. Therefore, in order to estimate the efficiency, the same detectors under test are used. The hit efficiency is defined as the ratio between the number of clusters in a detector for which the track extrapolated from the other two detectors matches the hit position[2] and the total number of tracks.

A cluster is considered as matched if the hit position is within 3 strips from the predicted position. Figures 11 show the dependence of the efficiency on the signal-to-noise ratio of the clusters and on the latency parameter.

---

[2] The hit position is defined as the charge weighted mean of the strips' position
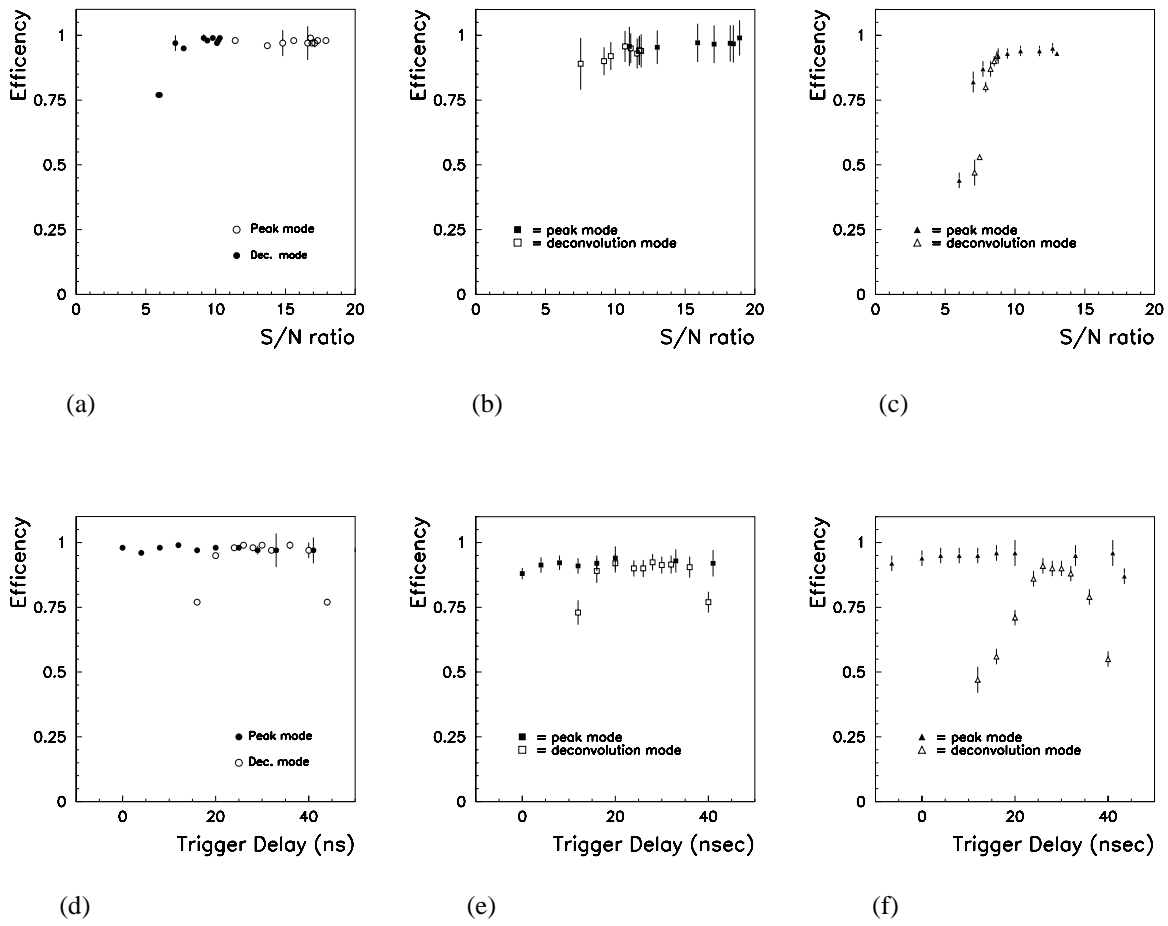
Figure 11: Efficiency vs S/N in peak and deconvolution mode for: (a) HR-NI, (b) LR-NI and (c) LR-IR. Efficiency vs latency delay in peak and deconvolution for: (d) HR-NI, (e) LR-NI and (f) LR-IR

For not irradiated detectors, both with high and low resistivity, in peak and deconvolution mode, the efficiency is greater than 95% for signal-to-noise ratios greater than 7. The irradiated detector reaches efficiencies of about 95%, for signal-to-noise ratios greater than 9. The latency parameter scan (figures d, e and f) shows a substantial independence of the efficiency on this parameter in peak mode, while in deconvolution mode the efficiency is contained within reasonable values only for a narrow window of the latency value. For the irradiated detector this window is considerably reduced, down to about 10 ns.

7 Conclusions

The performance on beam test of silicon microstrip detectors, with low (1-2 kΩ·cm) and high (4-8 kΩ·cm) resistivity, has been studied. One low resistivity detector was irradiated at a fluence $2.4 \cdot 10^{14}$ n/cm^2. The modules, with 12 cm strip length and 61 μm pitch, have been read-out with the APV6 chip, using both readout modes foreseen, peak and deconvolution. The high and low resistivity detectors before irradiation are found to be very similar in terms of signal-to-noise ratio and detection efficiencies. The low resistivity detectors have been successfully operated up to 500 V bias voltage. After irradiation, the low resistivity detector maintains a signal-to-noise ratio of about 9 at 400 V bias, in deconvolution mode, and assures an efficiency greater than 95%.

References

[1] CMS, The Tracker Project, Technical Design Report, CERN/LHCC 98-6 CMS TDR (1998).

[2] M.M Angarano, G.M. Bilei, M. Giorgi et al. *Characterization of neutron irradiated, low-resistivity silicon detectors*, CERN CMS C.R. 2000/06.

[3] D.Passeri, P. Ciampolini, G.M.Bilei *A Comprenensive Analysis of Low-Resistivity Silicon Radiation Detectors*, CERN CMS C.R. 1999/017.

[4] N. Marinelli, *APV logic simulation*, CERN CMS NOTE 1999/028.

[5] S. Gadomski, G. Hall et al. *The deconvolution method of fast pulse shaping at hadron colliders*, NIM A320 (1992) 217-227.

[6] W. Beaumont, *Crates Sincronization*, CERN web site.

[7] ORCA - website, http://cmsdoc.cern.ch/ORCA/

[8] M. French, *APV6 User Manual*, Rutherford Appleton Laboratory.

[9] C. Bozzi, *Signal-to-Noise evaluations for the CMS silicon microstrip detectors*, CERN CMS NOTE 1997/026

[10] M.M. Angarano, A. Bader, D. Creanza, M. de Palma, D. Diacono, S. My, G. Raso, P. Tempesta, *Characteristics and SPICE simulation of a single-sided, n^+ on n type Si strip detector before and after neutron irradiation*, CERN CMS NOTE 1998/34.